



An experimental study on mechanical properties of fiber-reinforced concrete of energy piles

Songying Zhao, Lei Chen

College of municipal and environmental engineering, Jilin Jianzhu University, China
coffeezy@163.com, 7796549@qq.com

Yan Fu

The First Construction Engineering Limited Company of China Construction Third Engineering Bureau, China
moonfuyan@foxmail.com

ABSTRACT. The technology of energy piles for heat storage involves turning the concrete piles buried beneath the ground into a part of the ground-source heat pump system and burying the heat-transfer tubes in the foundation piles, which are regarded as heat transfer wells. The heat transfer tubes are embedded in the concrete foundation piles, destroying the mechanical bearing capacity of the piles and damaging the safety of the buildings. Thus, considering the structural stability and the degree of heat transfer of concrete piles, as well as the selection of material for the foundation piles, the mixing ratio of the material of the energy piles is experimentally studied by the orthogonal method. The optimum mixing ratio of the energy pile is thus obtained. A concrete test block is used to conduct a static load test and splitting test to verify the mixing ratio of the concrete of the energy pile. The results show that steel fiber can be used to enhance the bearing capacity of the storage pile as a reinforcement material. Under a reasonable ratio, the reinforced pile can absolutely meet the original design requirements. Ordinary Portland cement or composite Portland cement can be used as cementitious materials for energy piles. Through an experiment, it is proved that the composite Portland cement can better meet the requirements of the concrete foundation piles than the cementitious material. As thermal conductivity materials, the addition of industrial graphite and scrap copper slag can improve the thermal conductivity of the pile, but it can also reduce the mechanical properties of the pile. It is necessary to control it in a certain range and not to add a large amount of graphite just to improve the thermal conductivity.

KEYWORDS. Energy pile; Mixing ratio; Fiber-reinforced material.



Citation: Zhao, S., Chen, L., Fu, Y., An experimental study on mechanical properties of fiber-reinforced concrete of energy piles, *Frattura ed Integrità Strutturale*, 41 (2017) 412-423.

Received: 14.03.2017

Accepted: 23.05.2017

Published: 01.07.2017

Copyright: © 2017 This is an open access article under the terms of the CC-BY 4.0, which permits unrestricted use, distribution, and reproduction in any medium, provided the original author and source are credited.

RESEARCH ON FIBER-REINFORCED CONCRETE OF ENERGY PILES

Principles of material selection

Figure 1 shows the load-strain curve of the non-tube pile and Figure 2 shows the load-strain curve of the buried pipes in the pile. It can be seen from the figures that if a heat transfer tube is buried in the pile, the concrete pile in the vicinity of the heat transfer tube is damaged more seriously, and the distribution of cracks is also very uneven, which indicates that after the heat transfer tube is buried, the compressive bearing capacity of the concrete pile foundation decreases greatly. After the heat transfer tube is buried in the pile foundation, the distribution of the strain curve of the pile is greatly changed, and the strain variation of the steel and the concrete is increased, which is more likely to cause the concrete pile to break [1-6].

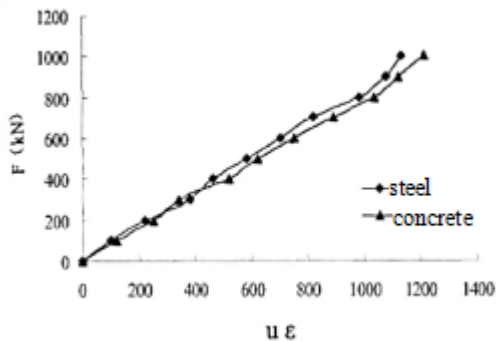


Figure 1: Load-strain curve of the non-tube pile.

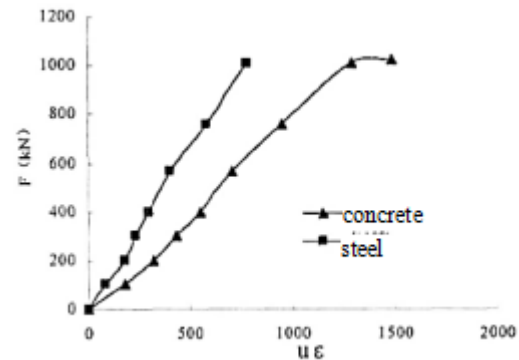


Figure 2: Load-strain curve of the buried tubes in the pile.

In addition, since the heat transfer tubes embedded in the concrete piles are to conduct the heat storage, a large amount of heat is stored in the energy piles, causing heat accumulation, which in turn causes the temperature of the center of the concrete piles to rise. When the concrete temperature rises to 100 °C, the internal free water begins to evaporate, and the chemical composition and physical structure of the concrete will change to about 500 °C [7-10]. Due to the decomposition of $\text{Ca}(\text{OH})_2$ leading to the concrete cracking, the concrete pile needs to remain at a high temperature to have favorable mechanical stability. Meanwhile, the expansion coefficient of the concrete materials is required to be as close to the expansion coefficient of the material of the heat transfer tube, so that it can effectively reduce the presence of an air film to avoid the unfavorable thermal conductivity of the pile.

Based on the analysis above, it is required that the selection of the concrete material of energy piles should meet the following conditions: firstly, the pile foundation of the building can still have stable mechanical properties at high temperature; secondly, the material of the pile foundation should have good thermal conductivity, so that the heat exchange can be conducted completely between the energy pile and soil; thirdly, the thermal expansion coefficient values of the heat transfer tubes and the concrete should be the same if possible to ensure that the heat transfer tubes and the concrete are tightly integrated without an air film, which would affect the thermal effect [11-15].

Choosing raw material

The main materials referred to in connection with the energy piles contain cement binders, aggregate, fiber, admixtures, and so on.

Kind of cement: composite Portland cement.

Type of coarse aggregate: basalt gravel with a density of $2.6 \times 10^3 \text{Kg/m}^3$.

Type of fine aggregate: natural sand; its modular and density are 2.6 and $2.55 \times 10^3 \text{Kg/m}^3$ respectively, its moisture content is 5%.

Type of fiber: the fiber-reinforced material mentioned here refers to steel fiber, whose length is 30-40 mm and whose tensile strength is 4500 MPa.

Type of material for storing heat: graphite and copper slag have a better thermal conductivity and the density of the graphite and copper slag in this experiment is $1.8 \times 10^3 \text{Kg/m}^3$ and $3.3 \times 10^3 \text{Kg/m}^3$ respectively.



Experimental study on mechanical properties of test piece of fiber-reinforced concrete

In this study, the compressive strength and anti-splitting strength of the test blocks are investigated by using the mixing ratio of the material in the concrete of the energy pile. The contents of fiber, graphite, copper slag, and fine aggregate are taken as the main factors, of which each factor is divided into three levels. This can be seen in Tab. 1.

Factor Level	A Carbon (steel) fibers (V%)	B Graphite(Kg/m ³)	C Copper slag (V%)	D Fine aggregate (V%)
1	0.0 (0.0)	0.0	0.0	0.0
2	0.25 (0.5)	1.0	2.0	2.0
3	0.5 (1.0)	2.0	4.0	4.0

Table 1: Factors and levels.

According to the factors and the levels, an L₉ (3⁴) orthogonal table is used, and the corresponding quality of each factor is determined to obtain orthogonal tests seen in Tab. 2.

Columns No. Test No.	A Carbon (steel) fibers(g)	B Graphite(g)	C Ordinary (Composite) copper slag (g)	D Ordinary (Composite) fine aggregate (g)
1	0(0)	0	0(0)	5.64(5.34)
2	0(0)	0.84	138.3(131.2)	5.53(5.20)
3	0(0)	16.8	276.5(262.4)	5.42(5.07)
4	37.8(372.6)	0	138.3(131.2)	5.53(5.20)
5	37.8(372.6)	0.84	276.5(262.4)	5.42(5.07)
6	37.8(372.6)	16.8	0(0)	5.64(5.34)
7	75.6(655.2)	0	276.5(262.4)	5.42(5.07)
8	75.6(655.2)	0.84	0(0)	5.64(5.34)
9	75.6(655.2)	16.8	138.3(131.2)	5.53(5.20)

Table 2: Orthogonal Test Table.

In the table, Ordinary refers to ordinary Portland cement and Composite means composite Portland cement. In this test, 2.97 kg of the ordinary Portland cement are used together with 1.78 kg of water. Moreover, 3.86 kg of composite Portland cement are mixed with 1.78 kg of water.

Experiment on mechanical properties of the concrete and results analysis

In accordance with the mixing ratio of the material in Tab. 2, 36 groups of test blocks of different mixing ratios are made. Each group with the same mixing ratio includes 6 blocks, which means 216 blocks are made in this experiment, which are to be used for the compressive strength and the anti-splitting experiments. The test results of the compressive strength are recorded in Tab. 3.

Figs. 3 and 4 show the relationship between the factors, the levels, and the K values in the compressive strength test when the ordinary Portland cement is used as the cementitious material and the carbon fiber and the steel fiber are selected as the fiber material. According to the conventional analysis of the orthogonal test, it can be seen that A is the carbon (steel) fiber, B is the graphite, and C is the scrap copper slag. In the course of the test, with the amount of these three materials increasing, the corresponding curves of the pile strength of K1, K2, and K3 can be seen in the figures.

In Fig. 3, in the case of A, for example, when the amount of fiber is increasing, the pile strength K1 to K3 are gradually reduced, and it can be concluded that when the content of this fiber increases, the compressive strength of the concrete is negatively impacted, and tends to decrease; the amount of B has little effect on the strength of the test blocks, and the strength slightly increases at Level 3. In Fig. 4, it can be intuitive to see that when the ordinary Portland cement is selected as the cementitious material, combined with the steel fiber in the reinforced experimental group, the strength does not significantly decrease when the steel fiber content increases, but slightly improves. According to the data, we can



see that the content of graphite in this experiment is the biggest factor affecting the strength, followed by scrap copper slag.

Numbering	Carbon fiber compressive strength test results (MPa)		Steel fiber compressive strength test results(MPa)	
	Ordinary Portland Cement	Composite Portland Cement	Ordinary Portland Cement	Composite Portland Cement
1	19.77	22.52	19.77	22.52
2	20.23	21.73	20.23	21.73
3	21.59	21.88	21.59	21.88
4	18.49	22.93	23.31	27.14
5	17.33	20.28	15.31	28.67
6	16.31	19.70	20.85	26.04
7	13.25	16.11	19.91	26.99
8	13.82	20.66	15.97	27.48
9	16.32	16.82	23.08	25.36

Table 3: Test results of the compressive strength.

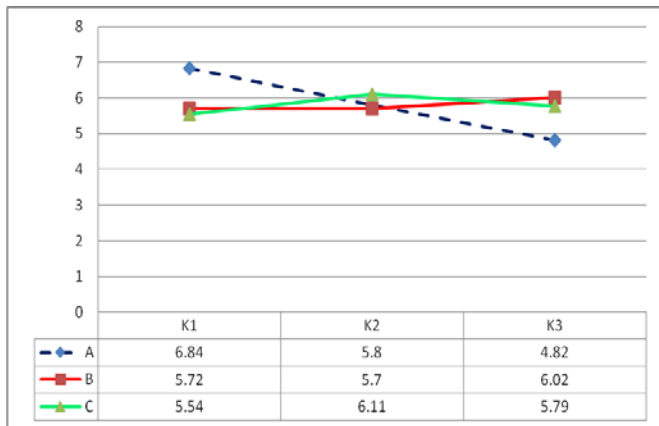


Figure 3: Relationship between the factors, the levels, and the K values (carbon fiber).

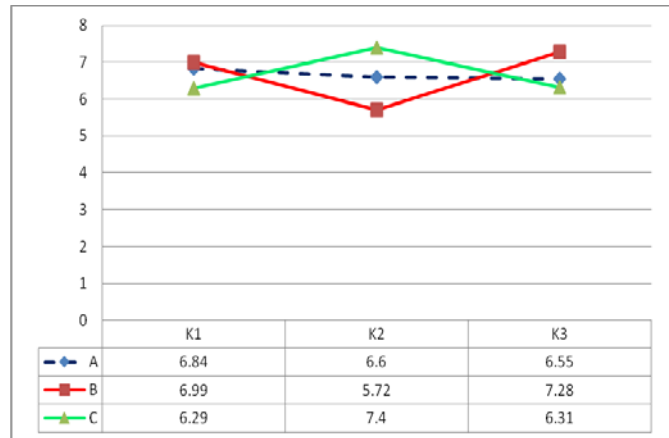


Figure 4: Relationship between the factors, the levels, and the K values (steel fiber).

Fig. 5 and Fig. 6 show the relationship between the factors, the levels, and the K values in the compressive strength test when the composite Portland cement is selected as the cementitious material, and carbon fiber and steel fiber are selected as the fiber materials.

It can be intuitively seen from Fig. 5 that when the composite Portland cement is selected as the cementitious material, combined with the carbon fiber in the reinforced experimental group, the strength decreases slightly when the content of the carbon fiber increases., meanwhile, the content of the carbon fiber impacts has a large impact on the concrete's strength largely, followed by the scrap copper slag, and the graphite has the smallest impact. Fig. 6 can be analyzed illustrates that when the content of the steel fiber is increased, the strength of the test block increases significantly. The amount of the steel fiber greatly affects the concrete strength largely, followed by the graphite, and the scrap copper slag has the smallest impact.

Tab. 4 shows the measured values of the anti-splitting strength of different material mixing ratios.

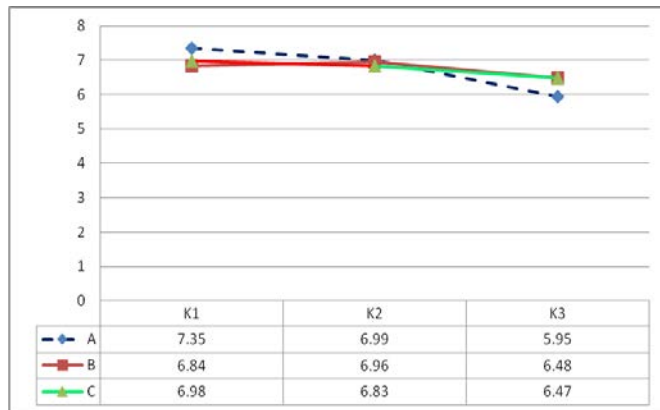


Figure 5: Relationship between the factors, the levels, and the K values (carbon fiber).

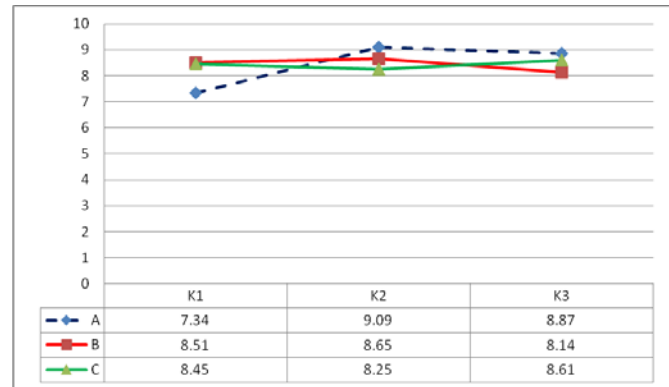


Figure 6: Relationship between the factors, the levels, and the K values (steel fiber).

Numbering	Carbon fiber compressive strength test results (MPa)		Steel fiber compressive strength test results (MPa)	
	Ordinary Portland Cement	Composite Portland cement	Ordinary Portland Cement	Composite Portland cement
1	41.54	50.16	41.54	50.16
2	42.72	47.91	42.72	47.91
3	43.45	46.70	43.45	46.70
4	50.81	43.64	56.42	45.10
5	40.30	38.34	37.84	56.72
6	40.25	37.26	34.26	53.42
7	43.57	40.56	40.70	47.40
8	40.73	48.24	34.75	56.14
9	43.10	46.60	36.89	54.42

Table 4: Anti-splitting test results.

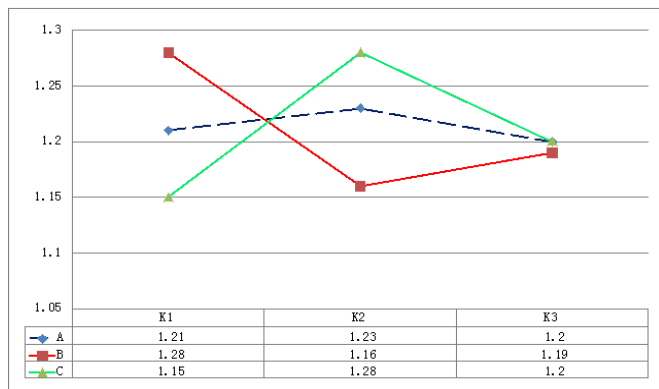


Figure 7: Relationship between factors, levels, and K values (carbon fiber).

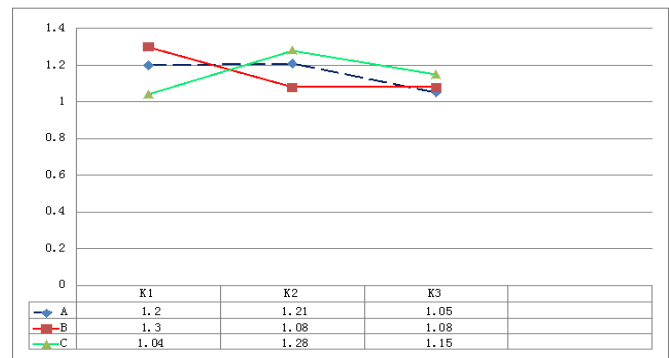


Figure 8: Relationship between factors, levels, and K values (steel fiber).



Fig. 7 and Fig. 8 show the relationship between the factors, the levels, and the K values of the anti-splitting test when the ordinary Portland cement is selected as the cementitious material and the carbon fiber and the steel fiber are selected as the fiber materials. It can be seen from Fig. 7 that the splitting strength clearly increases obviously when the content of the carbon fiber increases, and it declines when the content of the carbon exceeds a certain amount. Meanwhile, the content of the carbon fiber greatly affects the splitting strength of the concrete largely, followed by the graphite, and the scrap copper slag has the smallest impact. As can be analyzed concluded from Fig. 8, when the ordinary Portland cement is selected as the cementitious material, mixed with steel fiber in the splitting test group, with the amount of steel fiber increasing, the anti-splitting strength of the test block is basically even. According to the data in the figures, the content of graphite in this experiment is the biggest factor affecting the strength, followed by scrap copper slag.

Fig. 9 and Fig. 10 show the relationship between the factors, levels, and K values in the anti-splitting test when the composite Portland cement is selected as the cementitious material, and the carbon fiber and the steel fiber are selected as the fiber materials. It can be seen from Fig. 9 that the strength of the test block decreases slightly when the content of the carbon fiber increases, but it increases when the content of carbon exceeds a certain amount. It can be seen from Fig. 10 that the strength of the anti-splitting increases significantly when the content of the steel fiber increases, and the amount of the steel fiber greatly affects the concrete's strength largely.

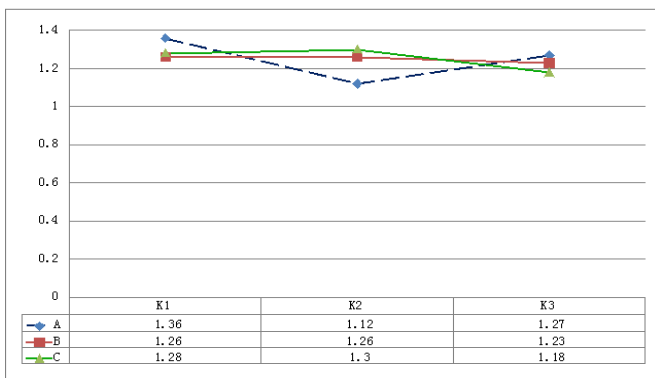


Figure 9: Relationship between factors, levels, and K values (carbon fiber).

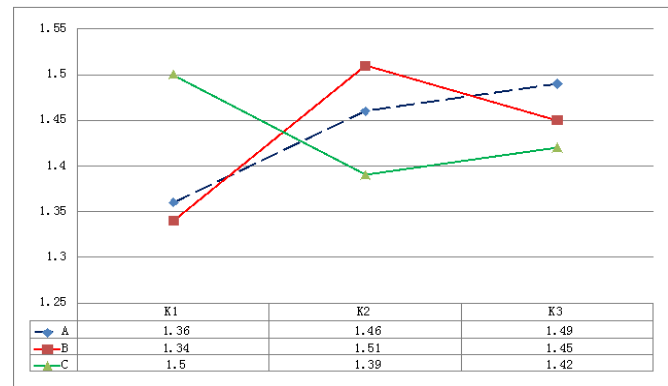


Figure 10: Relationship between factors, levels, and K values (steel fiber).

When comparing the compression process of the test blocks, it can be found that the pressure value of the concrete piece with carbon fiber under the pressure of the pressure testing machine of the concrete suddenly decreases, but the integrity of the test block is good. Under the pressure of the concrete pressure testing machine, the changes of in the compressive strength of the test block with steel fiber reflect are more uniform. However, after the test piece is damaged due to the pressure, the surface of the test block is more seriously damaged, as is shown in Fig. 11.



Figure 11: Damage situation of the two different test blocks after the pressure test

As can be seen from Fig. 11, (a) the compressive process of the ordinary concrete is clearer, and the pressure value decreases uniformly before the destruction, in line with the general law of the damage of the ordinary concrete; (b) the

concrete test block with the addition of carbon fiber cannot have better dispersion of the fiber in the mixing process, and the strength of the test block compared with the test block of ordinary concrete test block decreases significantly, the pressure value gets shows a rapid decline after reaching a certain point during the compressive process, but the test block body does not get suffer obviously damaged, retaining the its original shape well; (c) compared with the ordinary concrete, the strength of the steel fiber concrete is obviously improved, but the damage is more thorough and the damage interface is clearer from the macro observation.

From the analysis of the test data, it can be seen that the compressive strength and anti-splitting strength of the test blocks in the fifth group of materials are the largest in the orthogonal tests. That is, the composite Portland cement is used as the cementitious material, and the steel fiber is used as the reinforcement material. The ratio of the composition in each 20 kg of concrete can be seen in Tab. 5.

No.	Combination	Steel fiber(g)	Graphite (g)	Copper slag(g)	Fine aggregate(kg)	Coarse Aggregate(kg)	Cementations materials(kg)	Water (kg)
5	A ₂ B ₂ C ₃ D ₁	372.6	8.4	262.4	5.07	9.02	3.86	1.78

Table 5: Proportion Optimization Table

EXPERIMENTAL RESEARCH ON MECHANICAL PROPERTIES OF THE ENERGY PILES

Through the experimental ratio obtained by orthogonal experiments as well as the actual mixing process of each group, the composite Portland cement with steel fiber is selected to carry out the experiment with buried pipes in the piles, so as to further obtain the actual property indexes of the fiber- reinforced concrete of the energy piles.

Test plan

The test of mechanical properties of the energy piles is to involves testing the compressive strength of the pile body mainly through the static loading test of a pile. The heat-transfer tubes are supposed to be embedded in the energy piles, greatly weakening the vertical load of the foundation piles. This test is to verify the strength of the material of the energy piles so as to verify the correctness of the optimal ratio by conducting the pile loading without lateral force towards the energy piles through the compressive strength data and the damage mode of the piles.



Figure 12: Hydraulic pressure testing machine.



Figure 13: Preparation before the pile pile's static pressure.

In this test, three groups of concrete test piles are made and three identical concrete piles are made in for each set group. So, there are Nnine concrete piles are shared total in the test. As the standard pieces, the first group of the three concrete piles is the reinforced concrete piles with a normal ratio of material without reinforced fibers or embedded heat-transfer tubes. The second group of the three concrete piles is the reinforced concrete piles with a normal ratio of material with a group of single U-type heat-transfer tubes embedded in the piles, whose material is fits the PPR profile. The third group of the three piles is the energy piles whose material ratio is A₂B₂C₃D₁, with a group of single U-type heat-transfer tubes embedded in the piles, whose material is fits the PPR profile. The sizes of the test piles are that they have a diameter of

piles DN=200mm, and the length of the piles is 600 mm. The test piles adopt the concrete C30, the six main bars adopt the first-class steel bar whose diameter is $\varphi 8$, the stirrup is made of Wire No.8@200mm, the thickness of the protective layer of the concrete is 50 mm, the diameter of the heat-transfer tubes pre-embedded in the piles is DN=30mm, and the single U-shaped plastic pipes. The material ratio of the concrete piles in each group is shown in Tab. 6, Fig. 12 refers to the hydraulic pressure testing machine, and Fig. 13 shows the preparation before the pile's static pressure.

No.	Combination	Steel fiber(g)	Graphite (g)	Copper slag(g)	Fine aggregate (kg)	Coarse Aggregate (kg)	Cementitious materials(kg)	Water (kg)
1	First group	0	0	0	16.02	27.06	11.58	5.34
2	Second group	0	0	0	16.02	27.06	11.58	5.34
3	Third group	1117.8	25.2	787.2	15.21	27.06	11.58	5.34

Table 6: Material ratios of the test piles.

Test results and the analysis

The ultimate strength in of the three groups should be recorded respectively separately as collected in Tab. 7 when the foundation pile load is put on the upper part of the pile until the pile body is damaged, and Fig. 14 shows the damage situation of the foundation pile.

Category	No.	Group 1	Group 2	Group 3
Strength of the test pieces(KN)	1	375	311	382
	2	361	300	396
	3	345	285	373

Table 7: Ultimate strength of the test piles (kN).

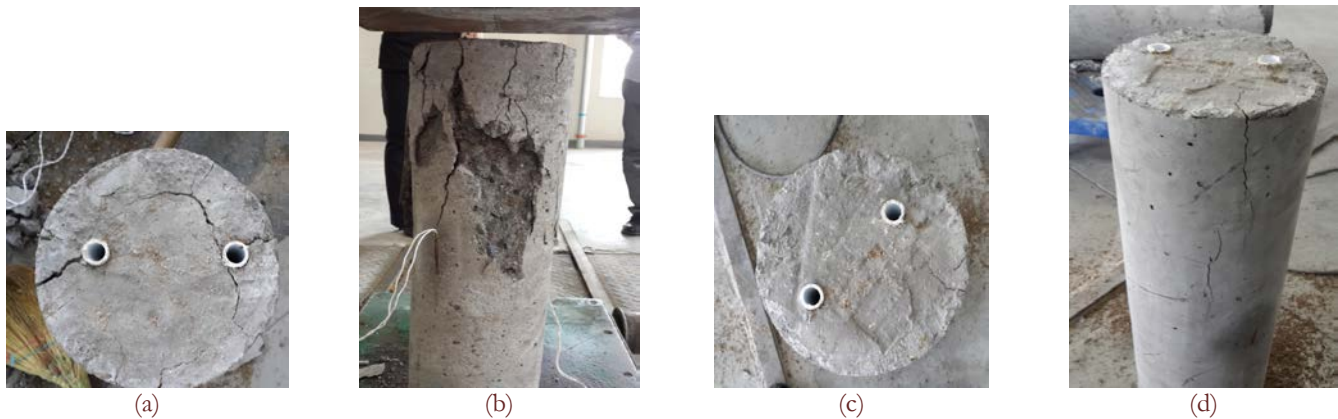


Figure 14: Damage situation of the pile body: (a) The end face of the pile with non-steel- fiber embedded pipes; (b) Non-steel- fiber pile without embedded pipes; (c) End face of the reinforced pile with steel fiber embedded pipes; (d) Reinforced pile body with steel fiber embedded pipes.

Fig. 14 shows the situation when the load is put on the upper part of the piles until the piles are damaged. The pile in Diagram a is a pile for burying the heat transfer tubes in the reinforced concrete piles. As can be seen from the damage, there are irregular cracks on the surrounding heat transfer tubes which are to be embedded, indicating that when the vertical load is carried out on the pile, the bearing capacity of the pile is affected due to by the irregular damage caused by reasons for the addition of the heat transfer tubes. The pile in Diagram b is the reinforced concrete pile under normal perfusion. The pile body is damaged due to the vertical load on it. Under the action of After the hydraulic pressure testing machine has been applied, cracks appear on the upper part of the concrete pile, and the concrete in the middle part of the pile breaks off, indicating that under the action of the vertical load force, the degree of the damage of to the pile is also serious. The piles in Diagrams c and Diagram d are the steel fiber- reinforced concrete piles with single U-shaped heat transfer tubes. It can be seen from Diagram c that although there are cracks on the top face of the pile, yet less but not as

many. Moreover, no obvious cracks can be found in the vicinity of the heat transfer tubes. After the application of the vertical load, the pile also cracks, but the concrete on it does not break off as what occurs in opposed to what occurred in Diagram b.

Fig. 15 shows the comparison between the test strength of the pile with buried pipes and the its theoretical strength. It can be seen from the figure that the theoretical strength of the second and third groups of test piles is supposed to be 97.5% of the theoretical strength of the first group. However, the test results show that the experimental strength of the second group of test piles with heat transfer tubes embedded in the concrete piles is only 47.8% of the theoretical strength. This result is far less than the result that the test strength is 58.8% of the theoretical strength in the first group of piles. The test group has a strength of 61.7% of the theoretical strength in the third group of teats piles with embedded heat transfer tubes with steel fiber. It can be verified by the experiment that the heat transfer tubes in the pile foundation can greatly reduce the compressive strength of the pile foundation, but the energy piles with the mixing ratio of A₂B₂C₃D₁ can improve the compressive strength of the pile foundation. The strength of the piles with the mixing ratio of A₂B₂C₃D₁ of the steel fiber, the heat storage material, and the thermal conductivity material will not be reduced, but improved to some extent.

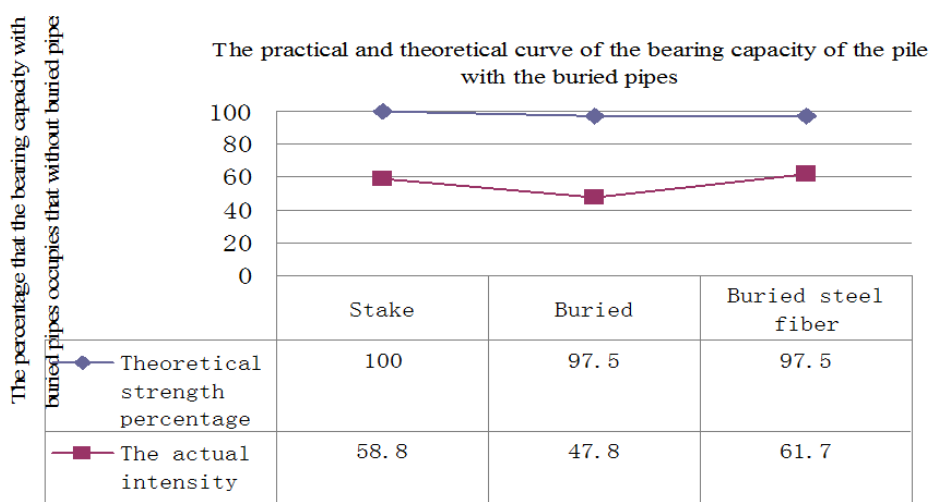


Figure 15: Comparison between the test of the pile with buried pipes and the its theoretical strength

The measurement of the thermal conductivity

The fourth group and the fifth group of the materials with the best compressive strength and the first group of the ordinary concrete materials are made as the test blocks to measure the thermal conductivity. The test blocks are made to be cuboid, the size of which is 0.03m × 0.1m × 0.1m. Three blocks are included in each test block, with a total of nine in this test. The evaporation of water of the test block is processed in the drying oven after its steel mold is taken out. The test block is taken out of the drying oven and the thermal conductivity is measured when the quality is kept constant. The main instruments for measuring the thermal conductivity are shown in Fig. 16, and the test results of the thermal conductivity are shown in Tab. 8.

As can be seen from Tab. 8, the thermal conductivity of the test blocks in the fourth and fifth group is improved greatly. The thermal conductivity of the block in Group 5 is over twice than that in Group 1, and the thermal conductivity of the block in Group 4 improves 1.5 times than that in Group 1.

The comparison of the heat storage capacity

The degree of the capacity of heat storage of the material is represented as the heat storage coefficient:

$$s = \sqrt{\frac{2\pi\lambda\rho c}{T}} \tag{1}$$

In the equation,

λ — the thermal conductivity of the material (W/m•K);

ρ — density of the dry matter of the material (kg/m³);



c — the specific heat of the material $J / (Kg \cdot K)$;
 T — time, 24 hours is set here.



(a) Drying oven



(b) Thermal conductivity tester

Figure 16: Main instruments for measuring the thermal conductivity

Group	Thermal conductivity(W/m.K)
Group 1	1.85
Group 4	2.81
Group 5	4.41

Table 8: Test results of thermal conductivity

The specific heat capacity of the concrete is:

$$c_p = \frac{\sum w_i c_i}{\sum w_i} \quad (2)$$

In the equation,

c_p — the specific heat capacity of the concrete $J / (Kg \cdot K)$

w_i — mass fraction of different parts

c_i — specific heat capacity of different parts

The specific heat capacity of different kinds of raw materials is: the specific heat capacity of the water is $4.186 \times 10^3 J / (Kg \cdot K)$; the specific heat capacity of the cement is $900 J / (Kg \cdot K)$; the specific heat capacity of the fine aggregate is $920 J / (Kg \cdot K)$; the specific heat capacity of the coarse aggregate is $850 J / (Kg \cdot K)$; the specific heat capacity of the steel is $450 J / (Kg \cdot K)$; the specific heat capacity of the graphite is $710 J / (Kg \cdot K)$; the specific heat capacity of the copper slag is $1060 J / (Kg \cdot K)$. It can be seen through calculation that the specific heat capacity of the first group of ordinary concretes is $1.175 \times 10^3 J / (Kg \cdot K)$, the specific heat capacity of the fourth group of the mixing material is $1.182 \times 10^3 J / (Kg \cdot K)$, the specific heat capacity of the fifth group of the mixing material $A_2B_2C_3D_1$ is $1.172 \times 10^3 J / (Kg \cdot K)$. With formula 1 added, it can be seen that the heat storage coefficient of the first group of materials is $19.3 W / (m^2 \cdot K)$, the thermal storage coefficient of the fourth group of materials is $24.47 W / (m^2 \cdot K)$, and the heat storage coefficient of the fifth group of materials is $30.6 W / (m^2 \cdot K)$. That is to say, the thermal storage capacity of the energy pile using a mixing ratio of $A_2B_2C_3D_1$ is 1.6 times than that of the ordinary reinforced concrete pile, whose effect of heat storage is relatively better.

CONCLUSION

1. Based on the mixing ratio of the material of the energy piles through the orthogonal test, the test piles made of the composite Portland cement with steel fiber are made, and the tests of the mechanical properties of the pile foundation are conducted to get the following conclusions:

2. The concrete test blocks with the addition of carbon fiber cannot have a good dispersion of the fiber in the mixing process, and the strength of the test blocks compared with that of the test blocks with containing ordinary concrete decreases significantly. The pressure value gets a decline rapidly decline after reaching a certain point during the compressive process, but the test blocks do not reflect obvious damage, and retaining their original shape. Compared with the strength of the ordinary concrete, the strength of the steel fiber- reinforced concrete increases significantly. But from a macroscopic observation, the destruction of the steel fiber concrete is more thorough, and the damage interface is relatively clear.
3. As the thermal conductivity materials, the addition of the industrial graphite and the scrap copper slag can improve the thermal conductivity of the pile, but it can also reduce the mechanical properties of the pile. It is necessary to control the amount within a certain range. It is infeasible not feasible to add too much graphite just to improve the thermal conductivity of the pile.
4. From an analysis of the experimental data analysis, the best- experimental program performing test group can be determined, which is the No. 5 test group with composite Portland cement selected as the cementitious material, and steel fiber as the reinforcement material, that is to say, the material. The material mixing ratio of the energy pile after optimization is $A_2B_2C_3D_1$.
5. The A static loading test is carried out towards on the three test piles. The results show that the effect of the heat transfer tubes on the compressive strength of the pile is far greater than the its theoretical influence. From According to the theoretical calculations data, the strength of the second group of test piles shall should be 97.5% of that of the first group of test piles. While Meanwhile in the static loading test, the strength of the second group of test piles is 80.7% of that of the first group of test piles. For the third group of piles with steel fiber, the result shows that the test strength of the piles in the third group is not only decreased, but also slightly improved, so as to which verifies the correctness of the material mixing ratio $A_2B_2C_3D_1$.
6. The thermal conductivity of the test blocks in the fourth and fifth group is improved greatly. The thermal conductivity of the block in Group 5 is over twice than that in Group 1; the heat storage coefficient of the first group of materials is $19.3 \text{ W} / (\text{m}^2 \cdot \text{K})$, the heat storage coefficient of the fifth group of materials is $30.6 \text{ W} / (\text{m}^2 \cdot \text{K})$. That is to say, the thermal storage capacity of the energy pile using a mixing ratio of $A_2B_2C_3D_1$ is 1.6 times than that of the ordinary reinforced concrete pile, whose effect of heat storage is relatively better.

ACKNOWLEDGMENTS

This work was supported by the National Natural Science Foundation of China (Grant No.51606084); Ji Lin Sheng Jiao Yu Ting Science and Technology Research [2016] (Grant No. 149); Ji Lin Sheng Ke Ji Ting QingNian Science and Technology Research [2016] (Grant No. 20160520028JH); Zhu Jian Bu Science and Technology Research [2016] (Grant No. 2016-K1-30).

REFERENCES

- [1] Denis, M., Philippe, P., The effect of borehole inclination on fluid and ground temperature for GLHE systems, *Geothermic*, 38(4) (2009) 392-398.
- [2] Zhan, N.Y., Xu, P.W., Influence of building envelop on natural convection and heat transfer when considering indoor heat transfer and radiation coupled in natural convection, *Acta Energiyae Solaris Sinica*, 32(4) (2011) 501-507.
- [3] Novoselac, A., Burley, B.J., Srebric, J., Development of new and validation of existing convection correlations for rooms with displacement ventilation systems, *Energy and Buildings*, 38(3) (2006) 163-173.
- [4] Franco, A., Moffat, R., Toledo, M., Herrera, P., Numerical sensitivity analysis of thermal response tests (TRT) in energy piles, *Renewable Energy*, 86 (2016) 985-992.
- [5] Caulk, R., Ghazanfari, E., McCartney, J.S., Parameterization of a calibrated geothermal energy pile model, *Geomechanics for Energy and the Environment*, 5 (2016) 1-15.
- [6] Brahim, T., Jemni, A., A Two-Dimensional Steady State Roll Heat Pipe Analyses for Heat Exchanger Applications, *International Journal of Heat and Technology*, 30(2) (2012) 115-119.
- [7] Peng, X., Natural ventilation and energy efficiency in building, *Industrial Construction*, 37(3) (2013) 5-9.
- [8] Singh, S.N., Flow and heat transfer studies in a double-pass counter flow solar air heater, *International Journal of Heat and Technology*, 31(2) (2013) 37-42.



- [9] Zhao, S.Y., Chen, C., Zhan, N.Y., Research on the influences of insulation technology by plastic greenhouses on working temperature in aeration tanks in cold areas in winter, *International Journal of Heat and Technology*, 32(1) (2015) 183-188.
- [10] Bensenouci, A., Benchatti, A., A Bounif A., Medjelledi, A., Study of the energy efficiency in building house using the DOE-2E and EE4 softwares simulation, *International Journal of Heat and Technology*, 27(2) (2009) 57-63.
- [11] Brandl, H., Energy foundations and other thermo-active ground structures, *Geotechnique*, 56(2) (2006) 81-122.
- [12] Go, G.H., Lee, S.R., Yoon, S., Kang, H.B., Design of spiral coil PHC energy pile considering effective borehole thermal resistance and groundwater advection effects, *Applied Energy*, 125(2) (2014) 165-178.
- [13] Zhao, S.Y., Su, X.S., Chen, C., Chen, L., An Application Study on the Simulative Optimization of the Ventilation of the Existing Buildings Based on CFD, *Revista De La Facultad De Ingenieria*, 31 (2016) 103-112.
- [14] Pinel, P., Cruickshank, C.A., Beausoleil-Morrison, I., Wills. A., A review of available methods for seasonal storage of solar thermal energy in residential applications, *Renew Sustain Energy Rev*, 15(7) (2011) 3341-3359.
- [15] Sekine, K., Okar, R., Hwang, S., Eng, M., Development of a ground-source heat pump system with ground heat exchanger utilizing the cast-in-place concrete pile foundations of buildings, *ASHRAE Transactions*, 113 (2007) 558–566.